Chemical Engineering Science 68 (2012) 424–431

Contents lists available at SciVerse ScienceDirect

Chemical Engineering Science

journal homepage: www.elsevier.com/locate/ces

Preparation and CO_2 adsorption of amine modified Mg–Al LDH via exfoliation route

Jiawei Wang [a,*], Lee A. Stevens [b], Trevor C. Drage [b], Joe Wood [a]

[a] School of Chemical Engineering, University of Birmingham, Birmingham B15 2TT, United Kingdom
[b] School of Chemical and Environmental Engineering, University of Nottingham, University Park, Nottingham NG7 2RD, United Kingdom

ARTICLE INFO

Article history:
Received 31 March 2011
Received in revised form
29 September 2011
Accepted 30 September 2011
Available online 12 October 2011

Keywords:
Adsorption
Carbon dioxide
Kinetics
Layered double hydroxide
Separation
Surfactant

ABSTRACT

In response to the recent focus on reducing carbon dioxide emission, the preparation and characterization of organically functionalized materials for use in carbon capture have received considerable attention. In this paper the synthesis of amine modified layered double hydroxides (LDHs) via an exfoliation and grafting synthetic route is reported. The materials were characterized by elemental analysis (EA), powder x-ray diffraction (PXRD), diffuse reflectance infrared Fourier transform spectrometer (DRIFTS) and thermogravimetric analysis (TGA). Adsorption of carbon dioxide on modified layered double hydroxides was investigated by TGA at 25–80 °C. 3-[2-(2-Aminoethylamino) ethylamino]propyl-trimethoxysilane modified MgAl LDH showed a maximum CO_2 adsorption capacity of 1.76 mmol g^{-1} at 80 °C. The influence of primary and secondary amines on carbon dioxide adsorption is discussed. The carbon dioxide adsorption isotherms presented were closely fitted to the Avrami kinetic model.

1. Introduction

The increasing atmospheric carbon dioxide concentration is of great concern to mankind, as it can be considered as a leading contributor to global climate change. The main cause for the increase of carbon dioxide concentration since the Industrial Revolution has been suggested to be due to man-made emissions (Hegerl et al., 2007). Among all carbon emission sources, fossil fuel power plants are one of the largest contributors to greenhouse gas emissions. Although amine solvent scrubbing technology is the most established technique available for post-combustion CO_2 capture in power plants, the associated energy penalty and cost make it less attractive economically. This has led to the development of alternative technologies to reduce the energy and cost penalty associated with carbon capture (Figueroa et al., 2008). Solid adsorbents could offer a potential route to significantly reduce the cost of CO_2 capture (Gray et al., 2008). According to Gray et al. (2008), the energy required for solid adsorbent based processes can be significantly lower than that of aqueous processes when the CO_2 adsorption capacity reaches or exceeds approximately 2 mmol g^{-1}. If the CO_2 adsorption capacity of solid adsorbents reaches 3 mmol g^{-1}, the energy reduction is estimated to be least 30–50% compared to the optimum aqueous monoethanolamine (MEA) based process. A range of porous materials have been explored with the key aim of developing materials with a high capacity and selectivity for CO_2 (Choi et al., 2009). Solid sorbent development for post-combustion capture has focussed on porous materials with modified surface chemistry to enhance adsorbent—CO_2 interaction under conditions of low CO_2 partial pressure. Possible techniques for enhancing the adsorption capacity include loading amines onto various types of supports such as mesoporous silicas, including SBA-12 (Zelenak et al., 2008), SBA-15 (Hiyoshi et al., 2005; Zelenak et al., 2008; Zukal et al., 2009), microspheres (Araki et al., 2009). Alternative supports include zeolites (Su et al., 2010; Zukal et al., 2009), MCM-41 (Zelenak et al., 2008) and MCM-48 (Huang et al., 2003; Kim et al., 2005). However grafting or impregnation are also feasible methods of preparation Scheme 1.

Layered doubled hydroxides (LDH), also known as hydrotalcite-like compounds, are composed of positively charged layers with charge balancing anions located in the interlayer region. LDH have the general formula $[M^{II}_{1-x}M^{III}_{x}(OH)_2][X^{q-}_{x/q}\cdot nH_2O]$ with x typically in the range between 0.10 and 0.33 (Forano et al., 2006). These materials can be readily and inexpensively synthesized with the desired characteristics for a particular application. LDH and calcined LDH (oxides) are widely used in the areas of catalysis, anion exchange and adsorption.

The use of LDH for adsorption of CO_2 has been investigated, but mainly under conditions of elevated temperature. Yong et al. (2001) reported several commercial hydrotalcite-like compounds

* Corresponding author. Tel.: +44 121 414 5081; fax: +44 121 414 5324.
E-mail address: j.wang.7@bham.ac.uk (J. Wang).

0009-2509
doi:10.1016/j.ces.2011.09.052

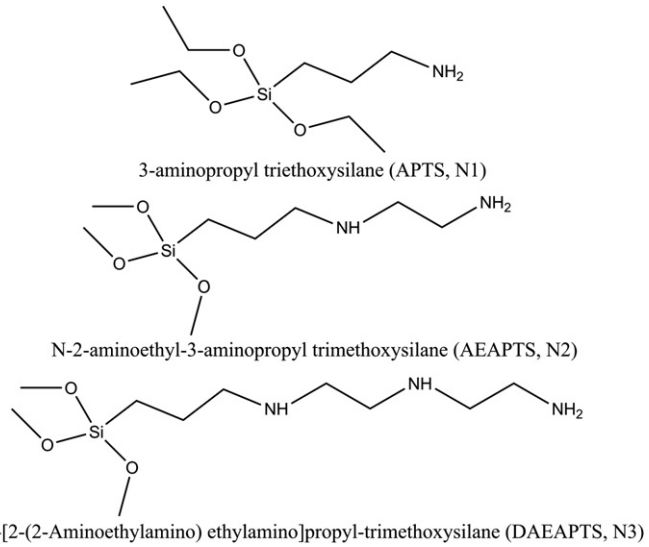

Scheme 1. Amine compounds used in the surface modification.

with adsorption capacities of 0.2–0.5 mmol g^{-1} at 300 °C and 1 bar of CO_2. They also found that the carbonate anion favours CO_2 adsorption compared to OH^-, and a low content of water can improve adsorption capacity. CO_2 adsorption capacities higher than 1.0 mmol g^{-1} have been reported by Hutson and Attwood (2008). A CO_2 adsorption capacity of 3.55 mmol g^{-1} was achieved by Ca–Al LDH with ClO_4^- anion at 330 °C and 1 bar. The adsorption capacity of LDH adsorbents can also be enhanced by promotion with potassium salts (Walspurger et al., 2008; Lee et al., 2007).

Amine modified LDHs have been prepared by several different methods. Park et al. (2005) used dodecyl sulfate (DS) intercalated LDH as precursor and added (3-aminopropyl)triethoxysilane (APTS) together with N-cetyl-N,N,N-trimethylammonium bromide (CTAB). The key step for the process was the formation of insoluble DS-CTAB salts and DS molecules were simultaneously replaced by APTS moieties. A process of exfoliation of LDHs followed by grafting of the single layers with aminosilanes has also been proposed (Wypych et al., 2005; Wypych and Satyanarayana, 2005). In-situ grafting of APTS onto the surface of LDHs with the assistance of DS was also reported by Tao et al. (2009a, b).

Compared with the widely studied LDH materials, reported investigations of CO_2 adsorption are lacking for amine grafted LDHs. The aims of this work were to prepare, characterize and for the first time evaluate the CO_2 adsorption capacity of amine modified LDH. In this work, amine modified Mg–Al LDHs prepared via an exfoliation route were characterized by Elemental Analysis (EA), Powder X-Ray Diffraction (PXRD), Diffuse Reflectance Infrared Fourier Transform Spectrometer (DRIFTS) and ThermoGravimetric Analysis (TGA). The exfoliation route was selected because of its higher exposure of surface hydroxyl group and lower diffusion limitation, which might lead to higher amine loading. The CO_2 adsorption behavior was investigated on these materials and the Avrami model was used to fit the adsorption kinetics.

2. Experimental

2.1. Preparation of DS intercalated LDH

The DS intercalated LDH was synthesized by the coprecipitation method of the relevant metal nitrates in DS solution. 4 g of $Mg(NO_3)_2 \cdot 6H_2O$ and 1.95 g of $Al(NO_3)_3 \cdot 9H_2O$ with a molar ratio of 3:1 (Mg^{2+}/Al^{3+}) were dissolved in 50 ml distilled water. The solution was added to a 3 g of sodium dodecyl sulfate dissolved in 100 ml distilled water, under vigorous stirring, at a rate of 0.5 ml min^{-1} at 70 °C. The pH value of the mixture was maintained at 10 by adding 4 M NaOH solution. The mixture was then aged for a further 4 h with the temperature and stirring maintained. The obtained material was filtered and washed with distilled water. The product was dried in a vacuum oven at 70 °C overnight.

2.2. Preparation of amine modified LDH

Aminosilanes were grafted on the LDH surface by the method reported by Wypych et al. (2005). In the method 0.5 g of DS intercalated LDH (MgAl DS) was added to a reaction flask containing 125 ml of toluene. The mixture was subjected to sonication in an ultrasound bath for 4.5 h at room temperature. After the suspension was kept for about 30 min, an extremely fine, white and voluminous gel formed at the bottom of the reactive flask.

The white gel was reacted with about 15 times the stoichiometric amount of aminosilanes under nitrogen atmosphere for 5 h at 60 °C. The precipitated solid was isolated by filtration and washed with toluene. Finally, the solid was dried under vacuum overnight. Three primary and secondary aminosilanes, 3-aminopropyl triethoxysilane (APTS), *N*-2-aminoethyl-3-aminopropyl trimethoxysilane (AEAPTS) and 3-[2-(2-Aminoethylamino) ethylamino]propyl-trimethoxysilane (DAEAPTS), were used. The corresponding samples were labeled as MgAl N1, MgAl N2 and MgAl N3. MgAl N*x* was used as a general designation for all three amine modified LDHs.

2.3. Characterization of the samples

Elemental analysis was performed using an Flash EA 1112 Elemental Analyzer (Thermo Electron S.p.A, Milan, Italy), configured to detect carbon, hydrogen, nitrogen and sulfur. The linear calibration method was selected using three calibration standards for accurate analysis: cystine, sulfanilamide and 2.5-(bis(5-tert-butyl-2-benzo-o-xazol-2-yl) (BBOT). Approximately 3 mg of sample (including standards) with 5 mg of vanadium pentoxide (V_2O_5) was sealed in tin capsules (8 × 5 mm) excluding air, and the samples were analyzed in triplicate. V_2O_5 was added to improve sulfur quantification.

PXRD patterns were collected using a Bruker-AXS D8 advance powder diffractometer with a scanning 2θ range of 2–65°. The basal spacing was calculated with Bragg's Law using the d_{003} and d_{006} peaks from the diffraction pattern.

DRIFTS were collected using a Bruker TENSOR 37 FTIR spectrometer with a diffuse reflectance accessory. KBr powder was used to collect background spectra. Spectra over the 4000–500 cm^{-1} range were collected with 64 scans and a resolution of 4 cm^{-1}. Samples were prepared by mixing the powdered solid with KBr in a ratio of 1:20. All samples were ground in a pestle and mortar and then sieved to ensure a consistent particle size of less than 75 μm.

In order to study the thermal decomposition of the samples, TGA was carried out in a mixture of N_2 and air from 25 to 1000 °C at a heating rate of 10 °C min^{-1} on a Netzsch TG 209 F1 thermogravimetric analyzer.

CO_2 adsorption was also measured by a Netzsch TG 209 F1 thermogravimetric analyzer. Approximately 5 mg of each sample was heated from 25 to 105 °C at 20 °C min^{-1} under N_2. The sample was held at 105 °C for 30 min and then cooled to the desired temperature at 10 °C min^{-1}. The gas input was switched from N_2 to CO_2 and held isothermally for 90 min. The CO_2 adsorption capacity was determined from the weight change in CO_2. Effects of the change in gas viscosity and gas density were

corrected by measuring the response to an empty platinum crucible by the same method.

CO_2 adsorption on liquid amine samples (APTS, AEAPTS and DAEAPTS) were also measured by TGA. About 20 mg liquid amine sample was placed in the platinum crucible and the temperature of the sample chamber was held isothermally at 25 °C for 10 min in N_2 to remove air from the system. The CO_2 was then introduced and the temperature was ramped to 200 °C at the rate of 10 °C min^{-1}.

3. Results and discussion

3.1. Characterization of amine modified LDH

3.1.1. Elemental analysis

Data from elemental analysis and PXRD are summarized in Table 1. The formula for intercalated and grafted molecules was calculated based on the elemental weight percentage of carbon, nitrogen and sulfur. The formula shows that MgAl DS had 1.87 mmol dodecyl sulfate anion per gram sample, and also captured 0.12 mmol nitrate and 1.04 mmol carbonate anions, which came from the metal salts used to prepare the samples and from atmospheric CO_2. The amount of dodecyl sulfate intercalated reduced to 1.42, 0.98 and 0.85 for MgAl DS N1, N2 and N3 after exfoliation and amine grafting, respectively. This indicates that dodecyl sulfate anions were partially replaced by amine silane molecules. It also shows that more DS anions were replaced with larger aminosilane molecules, which can be explained by the steric effect and larger molecules like DAEAPTS and AEAPTS occupy more space than APTS.

Based on elemental analysis data, the degree of silylation can also be calculated. Taking APTS as an example a general formula for grafted APTS moieties is $C_nH_{2.5n+0.5}NO_3Si$. When $n=9$, the formula is $C_9H_{23}NO_3Si$, which is the molecular formula of APTS. In this case there is no reaction between APTS molecules and the LDH layers. When $n=7.5$ or 3, correspondingly 1, 2 or 3 ethoxysilane groups react with hydroxyl groups on the LDH layers. Therefore, the degree of silylation reaction for MgAl DS N1 can be calculated from the formula (1):

$$\text{the degree of silylation} = \frac{9-n}{6} \times 100\%. \quad (1)$$

The same method can be applied to the other two aminosilanes.

As shown in Table 1, the MgAl N1 shows a degree of silylation of 98%, which means almost all ethoxysilane groups have attached to the LDH layers. MgAl N2 and MgAl N3, however, have only achieved 74% and 61% of the degree of silylation, respectively.

The amine loading (the number of moles of amine per total weight of material) is one of the most important parameters for CO_2 adsorbents, since the availability of basic amine groups influences the CO_2 uptake. MgAl N1, N2 and N3 had amine loading of 2.39, 5.14 and 6.01 mmol N g^{-1}, according to elemental analysis. Normalized by the number of amines in each silane, the actual number of silane molecules grafted for MgAl N1, N2 and N3 were 2.39, 2.57 and 2.00 mmol g^{-1}. The decrease in degree of functionalization was due to the size of the silane molecules (Choi et al., 2009). Larger silanes provide more steric hindrance and lead to smaller degree of surface functionalization.

3.1.2. PXRD

In Fig. 1, only PXRD patterns for MgAl DS and MgAl N3 are shown for clarity. All amine modified LDH samples have similar PXRD patterns apart from the peak positions of (003) and (006). The pattern for MgAl DS had the (003) and (006) reflections at 26.2 and 13.0 Å, corresponding to a basal spacing of 26.1 Å. The value was close to the previously reported values in the literature of 26.2 Å (Wypych et al., 2005) and 26.5 Å (Park et al., 2005; Tao et al., 2009a). As observed from Fig. 1, at the 2θ value equal to 60°, overlapping of the peaks corresponding to the (113) and (110) reflections occurred, which is usual for LDHs with large interlayer spacing (Herrero et al., 2009). After exfoliation and amine grafting, the sharpness and intensity of the reflections (003) and (006) reduced dramatically and a broad reflection was observed in the 2θ range of 15–30°. This indicates that the crystallinity of the system decreased after restacking of the layers. However, the non-basal reflections (012) and (110) were preserved, which indicates that the structure of the layers was conserved (Crepaldi et al., 2002).

The d-spacing was calculated as $[d_{(003)}+2d_{(006)}]/2$ (Herrero et al., 2009) and the values are listed in Table 1. MgAl N1, grafted with APTS, has a d-spacing of 24.1 Å, which was reduced from 26.1 Å of MgAl DS. As the size of grafted aminosilanes increased, the d-spacing of corresponding surface modified LDHs increased.

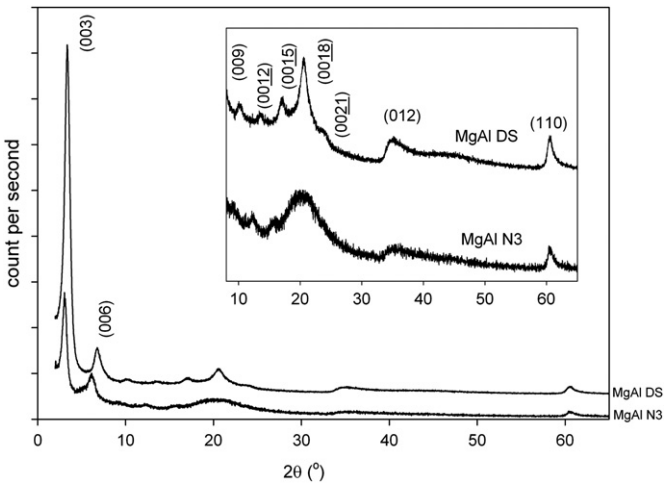

Fig. 1. PXRD patterns for samples MgAl DS and MgAl N3.

Table 1
Data of element analysis and PXRD.

Sample	Elemental weight (%)			Formula for intercalated and grafted molecules (mmol g^{-1})[a]	Degree of silylation	d spacing (Å)
	N	C	S			
MgAl DS	0.17	28.20	5.99	$(C_{12}H_{25}SO_4)_{1.87}(NO_3^-)_{0.12}(CO_3^{2-})_{1.04}$	–	26.1
MgAl N1	3.35	29.38	4.53	$(C_{12}H_{25}SO_4)_{1.42}(C_{3.13}H_{8.33}NO_3Si)_{2.393}$	98%	24.1
MgAl N2	7.20	32.04	3.15	$(C_{12}H_{25}SO_4)_{0.98}(C_{5.79}H_{15.37}N_2O_3Si)_{2.57}$	74%	28.5
MgAl N3	8.42	31.83	2.71	$(C_{12}H_{25}SO_4)_{0.85}(C_{8.16}H_{21.49}N_3O_3Si)_{2.01}$	61%	28.7

[a] To simplify data interpretation, it was assumed that all nitrogen, carbon and sulfur elements in the amine modified LDHs were only contributed from the intercalated and grafted organic molecules and nitrates and carbonates were ignored.

The *d*-spacing of MgAl N2 and N3 were increased to 28.5 and 28.7 Å, respectively. The increase of *d*-spacing implies the intercalation of grafted aminosilanes into LDH layers.

3.1.3. TGA

Fig. 2 shows the TGA and corresponding differential thermogravimetry (DTG) profiles of DS and amine modified LDHs. For DS intercalated LDH, the TGA profile shows four weight loss steps. The first one was from 25 to 150 °C with a total weight loss of 10.5%, attributed to the removal of surface adsorbed and interlayer water molecules (Tao et al., 2009a). The second step was from 150 to 300 °C with a decomposition peak at 224.8 °C in the DTG curve. A total weight loss of 31.1% was recorded during this step, which was thought to be related to dehydroxylation of LDH. Further dehydroxylation and dodecyl sulfate decomposition occurred over the temperature range from 300 to 850 °C with a total weight loss of 12.0%. The final step of 9.1% weight loss above 850 °C was attributed to the decomposition of the residual sulfate salt (Herrero et al., 2009).

When aminosilanes were bonded to the LDH surface, the thermal decomposition showed significantly different behavior. The most obvious difference was that the weight loss of MgAl N*x* in the process of dehydroxylation (150–300 °C) was much less than the one recorded in the sample of MgAl DS. This can be explained by the reaction of –OH group with silanol during grafting reaction (Tao et al., 2009a). It was followed by decomposition of alkyl chain in the temperature range of 300–850 °C with a total weight loss of about 50%. A further 8–9% weight loss was recorded at about 850 °C, corresponding to the residual sulfate salt decomposition, which was similar to the TGA of MgAl DS.

3.1.4. DRIFTS

The DRIFTS spectra of DS and amine modified LDHs are shown in Fig. 3. The spectrum of MgAl DS had a broad band in the region 3200–3700 cm^{-1}, which can be attributed to the stretching vibration of internal and hydrogen-bonded hydroxyl groups and adsorbed water molecules. The bending vibration of hydroxyl group also gave a band at 1634 cm^{-1}. The DS molecules showed a group of characteristic bands (Wypych et al., 2005) at 2955, 2920 and 2852 cm^{-1} (C–H stretching bond) and 1466 cm^{-1} (C–H bending bond) of the organic skeleton and at 1209, 1061 and 823 cm^{-1} ($-SO_4$). A band at 1382 cm^{-1} is attributed to nitrate ions, co-intercalated with DS (Crepaldi et al., 2002; Wypych et al., 2005). In the spectra of MgAl Nx, new bands related to N–H bonds were observed in the region of 3200 and 1570 cm^{-1}.

3.2. Adsorption of carbon dioxide

A typical TGA curve for CO_2 adsorption capacity measurement is shown in Fig. 4. At stage 1, the sample was pre-treated at 105 °C for 30 min under N_2. The weight loss at this stage was attributed to the loss of absorbed water. In stage 2 the sample was cooled to the required temperature for the CO_2 adsorption test. A slight weight gain was caused by N_2 adsorption on the sample. After the sample temperature was stable (stage 3), the gas input was switched to CO_2 and the associated weight gain was assumed to be due to the adsorbed CO_2.

Fig. 5 shows the CO_2 adsorption capacity of amine modified LDHs at four different temperatures, where each sample had the same pre-treatment as described above. The amount of carbon dioxide adsorbed on MgAl N1 was about 1.0 mmol g^{-1} in the

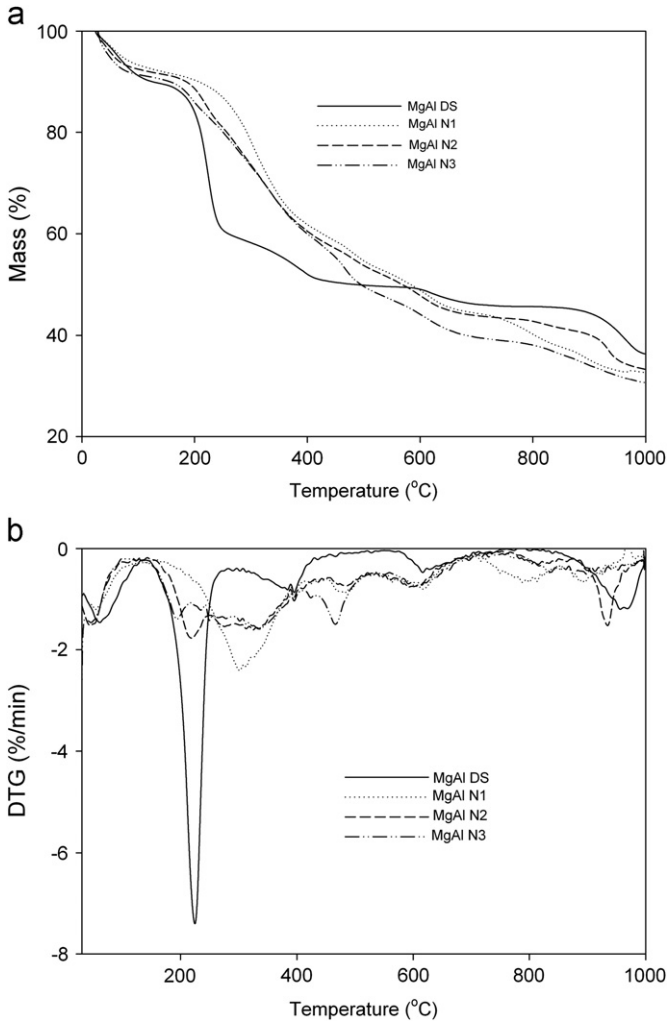

Fig. 2. TGA and DTG profiles of MgAl DS and MgAl N*x*.

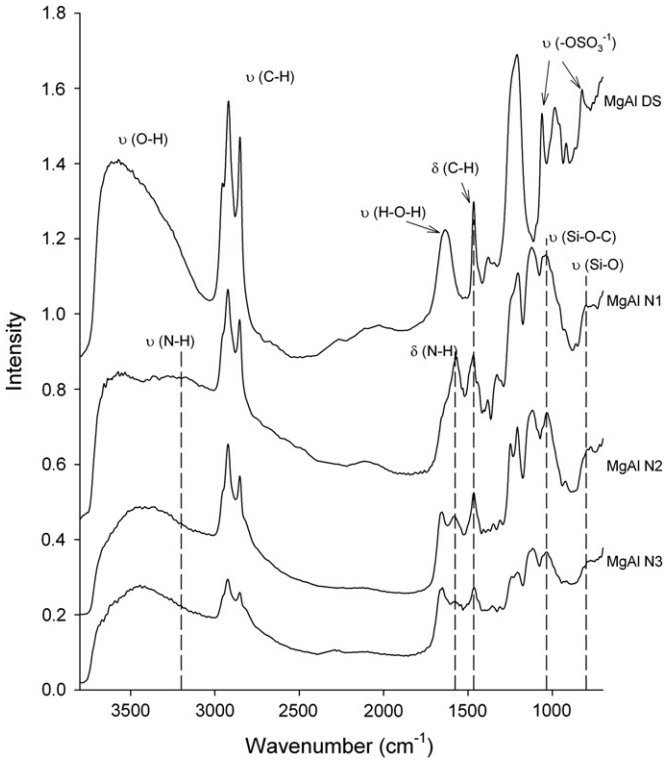

Fig. 3. DRIFTS spectra of DS and amine modified layered double hydroxides.

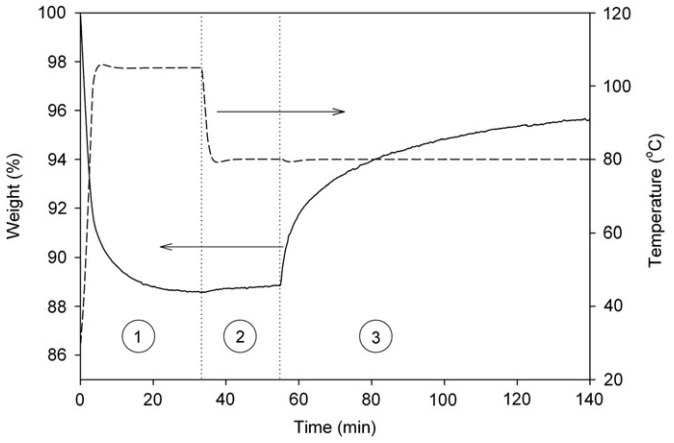

Fig. 4. A typical TGA curve for CO_2 adsorption capacity measurement.

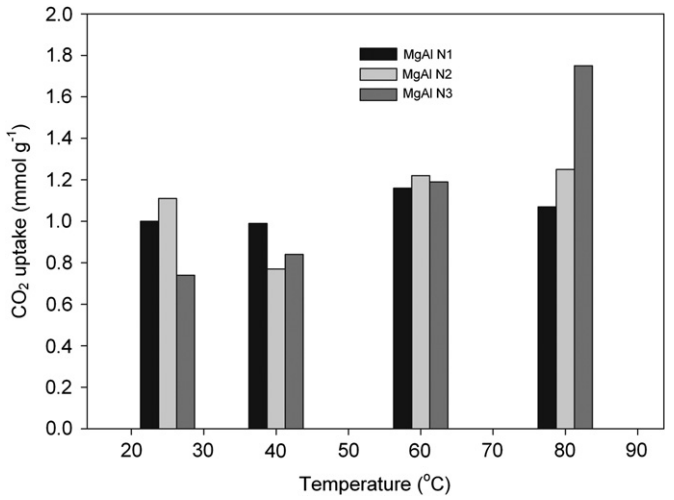

Fig. 5. CO_2 adsorption capacity of amine modified layered double hydroxides at 25, 40, 60 and 80 °C.

temperature range tested, which is within the range of values 0.57–2.05 mmol g^{-1} reported in the literature for CO_2 adsorption on APTES modified mesoporous silica (Hiyoshi et al., 2005; Huang et al., 2003; Zelenak et al., 2008). The amine efficiency is defined as the ratio of the amount of CO_2 adsorbed to the number of amine groups in the sample and thus provides a measure of how effective the grafted amines are in augmenting the adsorption capacity of the materials for CO_2. The amine efficiencies for the samples tested in this study were in the range of 0.41–0.48 mol CO_2 mol^{-1} N, which is close to the maximum efficiency of 0.5 based on carbamate formation mechanism (Satyapal et al., 2001). Under dry conditions, two moles of amine groups are required to remove every mole of CO_2 to form carbamate.

For the samples MgAl N2 and MgAl N3, the grafted aminosilanes not only have primary amine end groups, but also have secondary amines in their linkers. MgAl N2 had a CO_2 adsorption capacity of 1.1 mmol g^{-1} at 25 °C, which decreased to 0.8 mmol g^{-1} at 40 °C. At 60 and 80 °C, the CO_2 adsorption capacity increased to 1.2 mmol g^{-1}. Although the CO_2 adsorption capacity of MgAl N2 was higher than that of MgAl N1, the amine efficiency of MgAl N2 was in the range of 0.15–0.24, which was less than that of MgAl N1. The CO_2 adsorption capacity of MgAl N3 showed a steady increase from 0.74 mmol g^{-1} at 25 °C to 1.75 mmol g^{-1} at 80 °C. The trend is different from the previous results of hexagonal mesoporous silicas (HMSs) modified by DAEPTS, the same aminosilane used for preparation of MgAl N3, reported by Knowles et al. (2006). They reported that the CO_2 adsorption capacity of the DAEPTS modified HMS decreased from 1.34 mmol g^{-1} at 25 °C to 0.45 mmol g^{-1} at 75 °C. This suggests that positively charged MgAl brucite-like layers might affect CO_2 adsorption in a way which is different from silica based supports. The amine efficiency of MgAl N3 increased from 0.12 at 25 °C to 0.39 at 80 °C. Knowles et al. (2006) reported the AEAPTS and DAEAPTS modified HMSs had an amine efficiency of about 0.3. The authors suggested that the lower amine efficiencies than APTS modified HMS were due to reduced accessibility of CO_2 to the surface amine groups, as longer hydrocarbon chains might lead to reduced mobility and relative proximity of amine pairs. Comparing adsorption capacities in the current study with those reported in the literature, Lwin and Abdullah (2009) reported adsorption capacity of 30 mg g^{-1} (0.68 mmol g^{-1}) at 25 °C for CuAl-1.0 hydrotalcite, which decreased to 22 mg g^{-1} (0.5 mmol g^{-1}) at 150 °C. The adsorption of 0.74 mmol g^{-1} recorded in this study at 25 °C was only slightly higher than that measured by Lwin and Abdullah (2009), but the marked increase in adsorption that occurred with increasing temperature up to 80 °C in this work was in contrast with their study. This suggests that the amine modified adsorbents reported here would be useful in higher temperature capture processes, such as post-combustion capture.

To understand CO_2 adsorption of grafted amine at different temperatures, the CO_2 adsorption of three liquid amines was measured by TGA as well. The results are shown in Fig. 6. APTS showed a steady weight gain from 28 to 80 °C and started to lose weight at temperatures above 80 °C. This indicates that CO_2 begins to react with APTS from even the low temperature of 28 °C. However, AEAPTS and DAEAPTS showed very different behaviors for CO_2 uptake. While the weight gain for AEAPTS before 73 °C was slow compared to ATPS, it showed a sudden increase after that. Similar behavior was observed for DAEAPTS where the transition temperature at which the weight gained started to rapidly increase was 84 °C. The slower weight gain of AEAPTS and DAEAPTS at low temperature could be caused by their higher viscosity and therefore additional mass transfer limitation for CO_2 adsorption. The existence of transition temperature for AEAPTS and DAEAPTS suggests that primary amine sites and secondary amine sites have different initial reaction temperatures for CO_2 adsorption, as APTS has only primary amine sites and AEAPTS and DAEAPTS have primary and secondary amine sites.

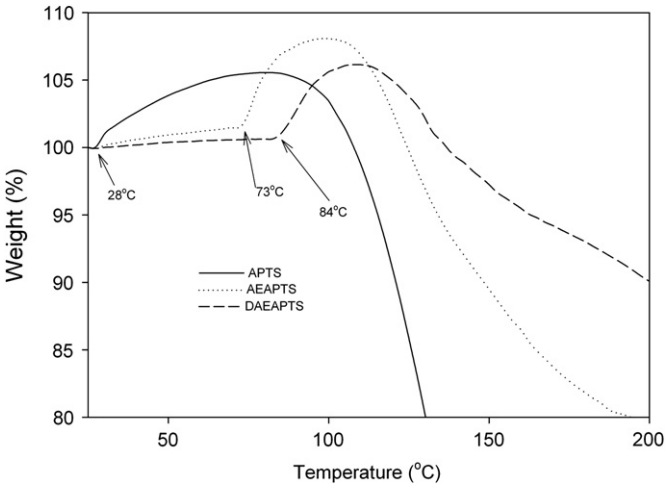

Fig. 6. TGA profiles of liquid aminosilanes under CO_2.

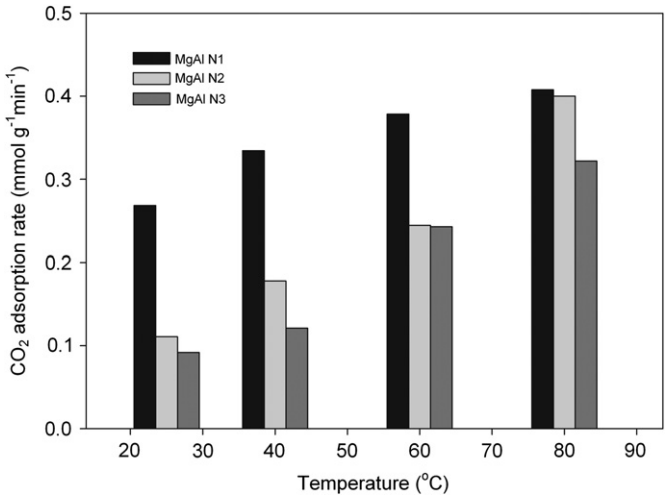

Fig. 7. CO_2 adsorption rate of amine modified layered double hydroxides at 25, 40, 60 and 80 °C.

Fig. 7 shows the initial CO_2 adsorption rate over each sample at different temperatures. For all three samples, the CO_2 adsorption rate increased with temperature. At every temperature tested, MgAl N1 always had the highest adsorption rate. This can be explained since the secondary amine has a slower reaction with CO_2 than primary amine (Harlick and Sayari, 2006). With increasing number of secondary amine sites, the CO_2 adsorption rate decreased in the order of MgAl N1 > MgAl N2 > MgAl N3. The adsorption rates reported by Lwin and Abdullah (2009) were strongly dependent upon temperature with CuAl-2.0 adsorbent displaying carbon dioxide adsorption rates in the range 1–16 mg g^{-1} min^{-1} (0.02–0.36 mmol g^{-1} min^{-1}) at 150–600 °C adsorption temperatures. However in this work, adsorption rates of up to 0.4 mmol g^{-1} min^{-1} were observed at the much lower temperatures, suggesting that the amine modified layered double hydroxides display a superior rate of adsorption.

3.3. Kinetic study

Kinetic information was obtained by isothermal adsorption of amine modified LDHs at different temperatures (i.e. 25, 40, 60 and 80 °C). The isothermal graphs of MgAl N*x* are presented in Fig. 8. All the isotherms of CO_2 adsorption were fitted by Avrami model (Avrami, 1939)

$$C_t = C_e[1-e^{-(k_A t)^{nA}}] \quad (2)$$

where C_t represents the amount of CO_2 adsorbed at time t, C_e is the amount of CO_2 adsorbed at equilibrium, k_A is the Avrami kinetic constant and n_A is the Avrami exponent. The Avrami model was used extensively to model phase transitions and crystal growth of materials (Jackson, 2004), and recently used to describe the adsorption of anionic dyes (Cestari et al., 2006) and CO_2 (Serna-Guerrero and Sayari, 2010) on amine-functionalized silicas. To determine the adequacy of the Avrami model fit to the adsorption data reported in this work, an error function based on the normalized standard deviation was calculated

$$Err(\%) = \sqrt{\frac{\sum[(C_{t(exp)}-C_{t(cal)})/C_{t(exp)}]^2}{N-1}} \times 100 \quad (3)$$

where Err (%) is the error function, $C_{t(exp)}$ is the experimental data of the amount of CO_2 adsorbed at time t, $C_{t(cal)}$ is the amount adsorbed as calculated by the Avrami model and N is the total number of experimental points.

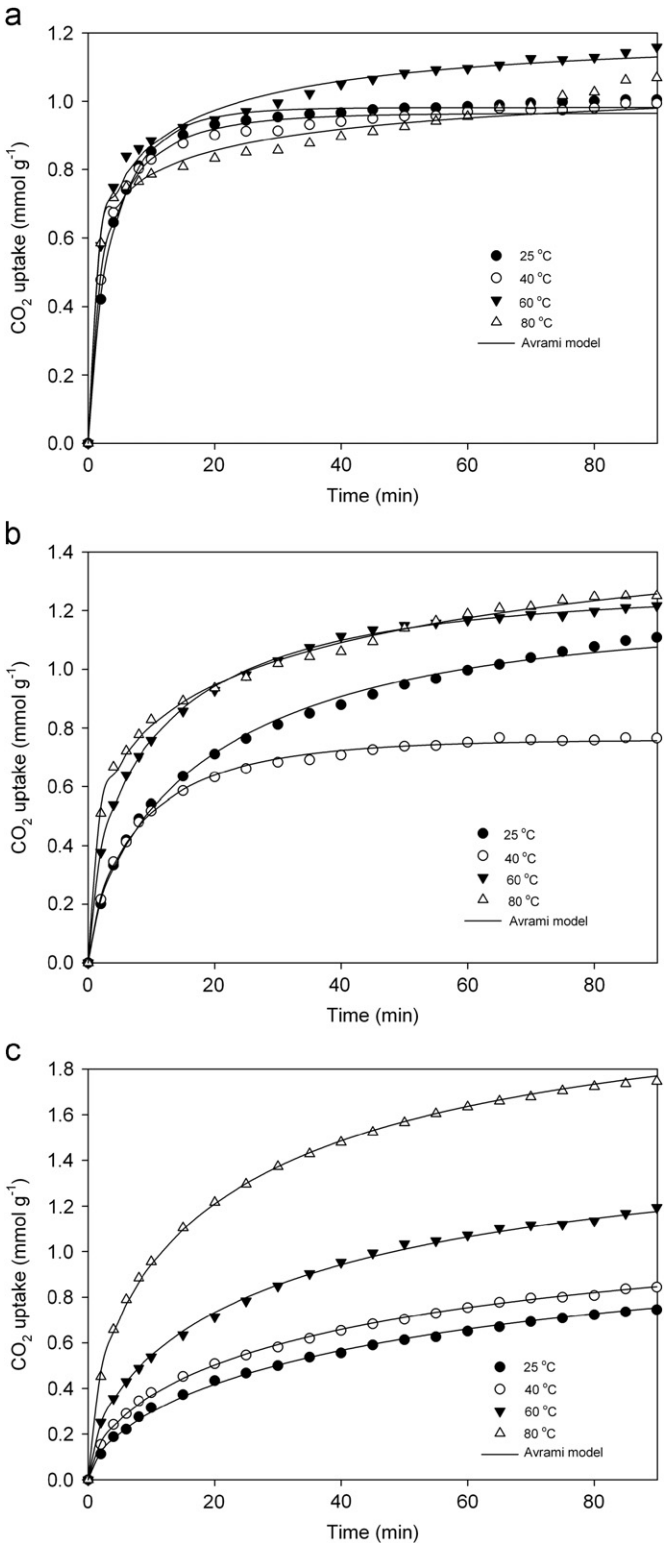

Fig. 8. Isotherms of CO_2 adsorption on MgAl N*x* at different temperatures. Experimental data are shown as points and Avrami model by curves. (a) MgAl N1, (b) MgAl N2, (c) MgAl N3.

For each isotherm, the values of C_e, n_A and k_A were calculated from experimental data through linear regression. The results are presented in Table 2. The calculated Avrami exponent for MgAl N2 varied from 0.79 at 25 °C to 0.27 at 80 °C. According to Cestari et al. (2006), the order of this model reflects the complexity of the reaction mechanisms or the occurrence of more than one reaction

Table 2
Kinetic parameters and error calculated from CO_2 adsorption isotherms fitted to Avrami model.

		25 °C	40 °C	60 °C	80 °C
MgAl N1	C_e (mmol g^{-1})	0.982	0.965	1.186	1.085
	n_A	0.79	0.63	0.38	0.27
	k_A (min^{-1})	0.335	0.464	0.555	0.692
	Err (%)	1.9	2.2	2.6	3.9
MgAl N2	C_e (mmol g^{-1})	1.161	0.760	1.261	1.674
	n_A	0.67	0.72	0.58	0.34
	k_A (min^{-1})	0.128	0.212	0.244	0.301
	Err (%)	2.8	1.9	1.1	1.9
MgAl N3	C_e (mmol g^{-1})	1.024	1.019	1.438	2.057
	n_A	0.62	0.58	0.58	0.53
	k_A (min^{-1})	0.082	0.107	0.126	0.181
	Err (%)	3.0	2.1	1.5	1.5

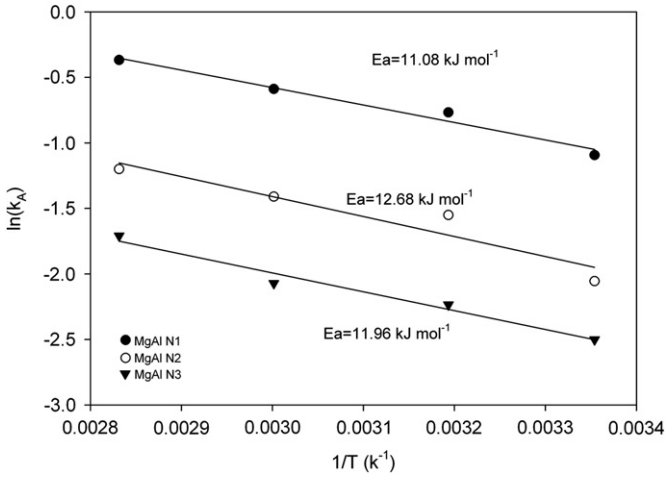

Fig. 9. Arrhenius plots for the kinetic constants obtained by Avrami model.

pathway. The decrease of Avrami exponent with temperature suggests that the adsorption of CO_2 seems to have less contact time dependence at elevated temperature.

The temperature dependence of the kinetic constant k_A may be described by the Arrhenius expression

$$k_A = Ae^{-(E_a/RT)} \tag{4}$$

where A is the Arrhenius pre-exponential factor, E_a is a term associated with the activation energy, R is the universal ideal gas constant and T is the absolute temperature. As shown in Fig. 9, the plots of natural logarithm of k_A against the reciprocal temperature show a reasonably linear trend for all three amine modified LDH. Therefore, E_a of CO_2 adsorption was calculated as 11.08, 12.68 and 11.96 kJ mol^{-1} for MgAl N1, MgAl N2 and MgAl N3, respectively. Serna-Guerrero and Sayari (2010) reported an E_a of 1.38 KJ mol^{-1} for CO_2 adsorption on triamine grafted mesoporous MCM-41 silica. However, the authors stated that caution must be applied if associating E_a with the actual activation energy in a semi-empirical model with a kinetic order other than unity. In this case, the Arrhenius equation is useful to predict k at different temperatures, while the other thermodynamic parameters are still debatable.

4. Conclusions

Amine modified LDHs have been synthesized via exfoliation and grafting route and studied as adsorbents for CO_2 at 25–80 °C. The materials were characterized by EA, PXRD, DRIFTS and TGA. It is the first time that CO_2 adsorption data has been reported for amine modified LDHs. The highest adsorption capacity for CO_2 was achieved at 1.75 mmol g^{-1} by MgAl N3 at 80 °C and 1 bar. The LDHs with only primary amine groups had the highest adsorption rate at any temperature. The Avrami model has provided a good experimental-simulation fit for the CO_2 adsorption isotherms on amine modified LDHs. The relatively high capacity at 80 °C together with favorable rates of adsorption make the amine modified layered double hydroxides suitable for use in post combustion carbon capture processes.

Notation

A	Arrhenius pre-exponential factor, min^{-1}
C_e	amount of CO_2 adsorbed at equilibrium, mmol g^{-1}
C_t	amount of CO_2 adsorbed at time t, mmol g^{-1}
$C_{t(exp)}$	experimental data of the amount of CO_2 adsorbed at time t, mmol g^{-1}
$C_{t(cal)}$	amount of CO_2 adsorbed at time t calculated by the Avrami model, mmol g^{-1}
E_a	activation energy, KJ mol^{-1}
Err	error function, %
k_A	Avrami kinetic constant, min^{-1}
n_A	Avrami exponent
N	total number of experimental points
T	absolute temperature, K

Acknowledgements

The authors acknowledge EPSRC and E.ON for financial support (E.ON-EPSRC strategic call on CCS Project EP/G061785/1).

References

Araki, S., Doi, H., Sano, Y., Tanaka, S., Miyake, Y., 2009. Preparation and CO_2 adsorption properties of aminopropyl-functionalized mesoporous silica microspheres. J. Colloid Interface Sci. 339, 382–389.
Avrami, M., 1939. Kinetics of phase change. I general theory. J. Chem. Phys. 7, 1103–1112.
Cestari, A.R., Vieira, E.F.S., Vieira, G.S., Almeida, L.E., 2006. The removal of anionic dyes from aqueous solutions in the presence of anionic surfactant using aminopropylsilica. A kinetic study. J. Hazard. Mater. B 138, 133–141.
Choi, S., Drese, J.H., Jones, C.W., 2009. Adsorbent materials for carbon dioxide capture from large anthropogenic point sources. ChemSusChem 2, 796–854.
Crepaldi, E.L., Pavan, P.C., Tronto, J., Valim, J.B., 2002. Chemical, structural, and thermal properties of Zn(II)–Cr(III) layered double hydroxides intercalated with sulfated and sulfonated surfactants. J. Colloid Interface Sci. 248, 429–442.
Figueroa, J.D., Fout, T., Plasynski, S., Mcilveried, H., Srivastava, R.D., 2008. Advances in CO_2 capture technology—The US Department of Energy's Carbon Sequestration Program. Int. J. Greenhouse Gas Control 2, 9–20.
Forano, C., Hibino, T., Lexoux, F., Taviot-Gueho, C., 2006. Layered double hydroxides. In: Bergaya, F., Theng, B.K.G., Lagaly, G. (Eds.), Handbook of Clay Science, Elsevier Science, Oxford, pp. 1021–1095.
Gray, M.L., Champagne, K.J., Fauth, D., Baltrus, J.P., Pennline, H., 2008. Performance of immobilized tertiary amine solid sorbents for the capture of carbon dioxide. Int. J. Greenhouse Gas Control 2, 3–8.
Harlick, P.J.E., Sayari, A., 2006. Applications of pore-expanded mesoporous silicas. 3. Triamine silane grafting for enhanced CO_2 adsorption. Ind. Eng. Chem. Res. 45, 3248–3255.
Hegerl, G.C., et al., 2007. Understanding and attributing climate change. In: Solomon, S., et al. (Eds.), IPCC Climate Change 2007, pp. 669–670.
Herrero, M., Labajos, F.M., Rives, V., 2009. Size control and optimisation of intercalated layered double hydroxides. Appl. Clay Sci. 42, 510–518.
Hiyoshi, N., Yogo, K., Yashima, T., 2005. Adsorption characteristics of carbon dioxide on organically functionalized SBA-15. Microporous Mesoporous Mater. 84, 357–365.
Huang, H.Y., Yang, R.T., Chinn, D., Munson, C.L., 2003. Amine-grafted MCM-48 and silica xerogel as superior sorbents for acidic gas removal from natural gas. Ind. Eng. Chem. Res. 42, 2427–2433.
Hutson, N.D., Attwood, B.C., 2008. High temperature adsorption of CO_2 on various hydrotalcite-like compounds. Adsorption 14, 781–789.

Jackson, K.A., 2004. Kinetic Processes: Crystal Growth, Diffusion, and Phase Transitions in Materials, 1st ed. Wiley-VCH, Weinheim.

Kim, S., Ida, J., Guliants, V.V., Lin, J.Y.S., 2005. Tailoring pore properties of MCM-48 silica for selective adsorption of CO_2. J. Phys. Chem. B 109, 6287–6293.

Knowles, G.P., Delaney, S.W., Chaffee, A.L., 2006. Diethylenetriamine[propyl (silyl)]-functionalized (DT) mesoporous silicas as CO_2 adsorbents. Ind. Eng. Chem. Res. 45, 2626–2633.

Lee, K.B., Verdooren, A., Caram, H.S., Sircar, S., 2007. Chemisorption of carbon dioxide on potassium-carbonate-promoted hydrotalcite. J. Colloid Interface Sci. 308, 30–39.

Lwin, Y., Abdullah, F., 2009. High temperature adsorption of carbon dioxide on Cu–Al hydrotalcite derived mixed oxides: kinetics and equilibria by thermogravimetry. J. Therm. Anal. Calorim. 97, 885–889.

Park, A.Y., Kwon, H., Woo, A.J., Kim, S.J., 2005. Layered double hydroxide surface modified with (3-aminopropyl)triethoxysilane by covalent bonding. Adv. Mater. 17, 106–109.

Satyapal, S., Filburn, T., Trela, J., Strange, J., 2001. Performance and properties of a solid amine sorbent for carbon dioxide removal in space life support applications. Energy Fuels 15, 250–255.

Serna-Guerrero, R., Sayari, A., 2010. Modeling adsorption of CO_2 on amine-functionalized mesoporous silica. 2: Kinetics and breakthrough curves. Chem. Eng. J. 161, 182–190.

Su, F., Lu, C., Kuo, S.C., Zeng, W., 2010. Adsorption of CO_2 on amine-functionalized Y-type zeolites. Energy Fuels 24, 1441–1448.

Tao, Q., He, H., Frost, R.L., Yuan, P., Zhu, J., 2009a. Nanomaterials based upon silylated layered double hydroxides. Appl. Surf. Sci. 255, 4334–4340.

Tao, Q., Yuan, J., Frost, R.L., He, H., Yuan, P., Zhu, J., 2009b. Effect of surfactant concentration on the stacking modes of organo-silylated layered double hydroxides. Appl. Clay Sci. 45, 262–269.

Walspurger, S., Boels, L., Cobden, P.D., Elzinga, G.D., Haije, W.G., van den Brink, R.W., 2008. The crucial role of the K^+-aluminium oxide interaction in K^+-promoted alumina- and hydrotalcite-based materials for CO_2 sorption at high temperatures. ChemSusChem 1, 643–650.

Wypych, F., Bail, A., Halma, M., Nakagaki, S., 2005. Immobilization of iron(III) porphyrins on exfoliated MgAl layered double hydroxide, grafted with (3-aminopropyl)triethoxysilane. J. Catal. 234, 431–437.

Wypych, F., Satyanarayana, K.G., 2005. Functionalization of single layers and nanofibers: a new strategy to produce polymer nanocomposites with optimized properties. J. Colloid Interface Sci. 285, 532–543.

Yong, Z., Mata, V., Rodrigues, A.E., 2001. Adsorption of carbon dioxide onto hydrotalcite-like compounds (HTlcs) at high temperatures. Ind. Eng. Chem. Res. 40, 204–209.

Zelenak, V., Badanicova, M., Halamova, D., Cejka, J., Zukal, A., Murafa, N., Goerigk, G., 2008. Amine-modified ordered mesoporous silica: effect of pore size on carbon dioxide capture. Chem. Eng. J. 144, 336–342.

Zukal, A., Dominguez, I., Mayerova, J., Cejka, J., 2009. Functionalization of delaminated zeolite ITQ-6 for the adsorption of carbon dioxide. Langmuir 25, 10314–10321.